Biophysical Chemistry, 48 (1994) 359–368
Elsevier Science B.V., Amsterdam

BIOCHE 01794

Interaction of TNP–ATP with tubulin: A fluorescence spectroscopic study

Sadananda S. Rai and Sitapati R. Kasturi *

Tata Institute of Fundamental Research, Homi Bhabha Road, Colaba, Bombay 400005 (India)

(Received 3 March 1993; accepted in revised form 1 July 1993)

Abstract

The interaction of the ribose-modified ATP analogue, 2′(or 3′)-*O*-(2,4,6-trinitrophenyl)adenosine 5′-triphosphate (TNP–ATP) with tubulin has been examined using fluorescence techniques. It has been found that TNP–ATP inhibits the polymerization of tubulin and it binds to tubulin at a site distinct from that of GTP or ATP with a stoichiometry of 1:1 and dissociation constant of 110 ± 15 μM. Tubulin-bound TNP–ATP fluorescence is quenched by ANS implying that TNP–ATP binds in the vicinity of the ANS binding site. Further, TNP–ATP quenches the tryptophan fluorescence of the protein, suggesting the proximity of the TNP–ATP binding site to tryptophan residues. A significant upfield shift for the proton resonances of the trinitrophenyl ring and for the ribose protons of TNP–ATP has been observed in the NMR spectra. These NMR results show that the nitrogroup and sugar moiety of TNP–ATP interact with the protein. From these results, it appears that the binding site of TNP–ATP is critical for polymerization.

Keywords: Tubulin; Ligand binding; TNP–ATP; Inhibition; Interaction

1. Introduction

The interaction of guanine nucleotide with tubulin, the major structural protein of microtubules, has been studied extensively in many laboratories. The tubulin dimer binds two moles of guanine nucleotide [1], one binding at the exchangeable site (E-site) where it exchanges with the exogenous nucleotide and the other at the non-exchangeable site (N-site) where it does not exchange [2]. A number of investigators have also examined the effect of ATP on microtubule assembly in vitro [3–7]. Zabrecky and Cole reported that ATP induces the microtubular assembly [3]. In order to study the effect of ATP on microtubule assembly and the nature of its interaction with tubulin using fluorescence spectroscopy, it would be of particular importance to synthesize fluorescent analogues of the nucleotide. The ribose-modified fluorescent analogues of the adenine nucleotide, (TNP-ATP) and (Ant-ATP), have been used to probe the nucleotide binding sites of a number of ATPases [8–11]. The fluorescence

* To whom correspondence should be addressed. Tel.: 091-22-2152971; Fax: 091-22-2152110; Telex: 011-83009 TIFR IN.

Abbreviations: TNP–ATP, 2′ (or 3′)-*O*-(2,4,6-trinitrophenyl) adenosine 5′-triphosphate; Ant–ATP, 3′-*O*-anthraniloyladenosine 5′-triphosphate; Pipes, 1,4-piperazinediethanesulphonic acid; SDS, sodium dodecyl sulphate; ANS, 8-anilino-1-napthalenesulphonic acid.

SSDI 0301-4622(93)E0048-A

of the bound analogue has been shown to increase severalfold and this enhancement in fluorescence can be used to study the interaction between the nucleotides and the protein.

In this study, we have examined the role of TNP–ATP on tubulin self-assembly and the effect of other ligands which bind to tubulin on the bound TNP–ATP.

2. Materials and methods

All chemicals were obtained from Sigma Chemical Co. (St. Louis, MO, USA) unless otherwise mentioned.

2.1. Isolation and purification of tubulin

Tubulin was isolated from fresh goat brains by a modification of the procedure of Shelanski et al. [12] using cycles of assembly and disassembly in a buffer containing 0.1 *M* Pipes, pH 6.9, 1 m*M* $MgCl_2$, 2 m*M* EGTA, 8 *M* glycerol, 1 m*M* GTP. Tubulin was purified from microtubule-associated proteins by chromatography on phosphocellulose (Whatman P-11) column equilibrated with buffer (0.1 *M* Pipes, pH 6.9, 1 m*M* $MgCl_2$, 2 m*M* EGTA, 0.1 m*M* GTP). The tubulin fractions were collected and concentrated using Amicon CF50A membrane cones. Purity was checked by Coomassie Blue-stained SDS gel electrophoresis and was found to be about 98% pure. Protein was estimated by Lowry method [13] and was stored at −80°C, until used.

2.2. Preparation of ATP analogue

TNP–ATP was prepared according to the method of Hiratsuka and Uchida [14]. 1 gram of ATP was dissolved in 10 ml of water at 30°C. The pH of the solution was kept at 9.5 with the addition of NaOH. To this solution 34 ml of picryl sulfonic acid (5% w/v) was added dropwise with constant stirring and adjusting the pH to 9.6. The reaction was allowed to complete for two hours with stirring. The derivative was washed several times with ethanol in which the nucleotide precipitated. The compound was dissolved in water and neutralized to pH 7.0 with 1 *N* HCl. The solution was loaded onto a Sephadex LH-20 column (2.0 × 60 cm) equilibrated with water. Column was eluted with water and fractions of 3 ml were collected. Unreacted ATP was eluted first. The TNP–ATP fractions were collected and lyophilized to get the solid form. Purification was repeated until the pure form was obtained. Purity of this analogue was checked by HPLC using C-18 reverse phase column and was found to be at least 99% pure. The compound was characterized by absorbance, emission and NMR spectra.

TNP–ATP synthesized by us has absorption maxima at 259 nm ($\epsilon = 25000\ M^{-1}\ cm^{-1}$), 408 nm ($\epsilon = 26400\ M^{-1}\ cm^{-1}$) and 470 nm ($\epsilon = 18500\ M^{-1}\ cm^{-1}$) at pH 8.0, in agreement with the earlier workers [14]. It has fluorescence emission in the range of 540 nm when excited with light of 410 nm.

2.3. Polymerization study

Polymerization experiments in the presence of ATP were carried out under the conditions used by Zabrecky and Cole [3] (10 m*M* Pipes, 5 m*M* $MgCl_2$, 1.0 m*M* EGTA, 3.4 M glycerol) at pH 6.4, 4°C). Polymerization was initiated by adding the appropriate nucleotide and then warming to 37°C in a thermostatically controlled cuvette chamber of Milton Roy spectrophotometer (Model 1201). The increase in turbidity was monitored at 350 nm. Tubulin dimer concentrations used for the polymerization experiments are shown in the figures. The path length was 1 cm.

2.4. NMR study

For NMR experiments, protein and ligand solutions were passed through Chelex-100 which was previously washed with acid and equilibrated to pH 7.0 with 20 m*M* Pipes prepared in deionized water. For ^{1}H-NMR, final protein samples were in 20 m*M* Pipes, pH 7.0. The samples were then lyophilized and dissolved in D_2O which is used as an internal lock. ^{1}H-NMR spectra were recorded at 500 MHz Bruker AMX-500 NMR spectrometer. Proton chemical shifts were mea-

sured relative to the internal reference sodium 3-trimethylsilyl-(2,2,3,3-$^2H_4$)propionate. All samples for ^{1}H-NMR were placed in 5-mm NMR sample tubes (Wilmad Glass Company Inc., New Jersey, USA) and measurements were made at 25°C. Measurements in the presence of the protein were completed within two hours after the preparation of the sample.

2.5. Steady state fluorescence measurements and analysis of data

Steady state fluorescence experiments were carried out using Shimadzu fluorimeter (Model RF-540). Excitation and emission slits were 5 nm and 10 nm, respectively. In order to minimise the inner-filter effect, TNP–ATP was excited at 480 nm and the emission was recorded from 500 nm to 600 nm. The inner-filter effect was corrected according to the procedure given by Lakowicz [15].

The binding constant and stoichiometry were calculated from the following equation:

$$\frac{F_0}{F-F_0} = \frac{K_d}{Q}\frac{1}{[P]} + \frac{1}{Q}, \tag{1}$$

where F and F_0 are the observed fluorescence of the fluorescent analogue in the presence and absence of the protein, respectively; K_d is the dissociation constant of the complex and [P] is the free protein concentration. The fluorescence enhancement factor, Q is defined as

$$Q = \frac{F_{bound}}{F_{free}} - 1, \tag{2}$$

where F_{bound} and F_{free} are the fluorescence intensities of the ligand in the fully bound and the free form, respectively. The enhancement factor Q can be obtained from the intercept of the linear plot of $F_0/(F-F_0)$ vs. $1/[P]$ with the assumption that $[P] = [P]_{total}$, at sufficiently high excess of protein with respect to the dissociation constant for the protein-ligand complex. Once the value of Q is known, the concentration of the bound ligand, [EL], can be calculated from a fluorescence titration experiment such as

$$[EL] = \frac{F_{total} - \phi[L]_T}{\phi Q}, \tag{3}$$

where F_{total} is the total TNP–ATP fluorescence minus blank in the presence of the protein, $[L]_T$ is the total TNP–ATP concentration, and ϕ is the quantum yield of free TNP–ATP given by

$$\phi = F_{free}/[L]. \tag{4}$$

The stoichiometry of binding can be calculated from the value of EL thus determined (eq. 3) and using the Klotz equation [16] given below,

$$\frac{1}{\bar{\nu}} = \frac{K_d}{n}\frac{1}{[L]} + \frac{1}{n}, \tag{5}$$

where $\bar{\nu}$ is the ratio of the concentration of bound ligand ([EL]) to the total protein concentration $[P]_t$, n represents the number of binding sites per protein, [L] is the concentration of free ligand, and K_d is the dissociation constant of the tubulin–TNP–ATP complex.

2.6. Temperature dependence of the dissociation constant (K_d)

The K_d for binding of TNP–ATP to tubulin was determined fluorometrically in the temperature range 15°C to 35°C. The results are plotted in the form of the Van't Hoff equation

$$\ln K_d = \frac{\Delta H^0}{RT} - \frac{\Delta S^0}{R} \tag{6}$$

The enthalpy change (ΔH^0) and the entropy change (ΔS^0) are obtained from this plot. The change in free energy ΔG^0 at any temperature can be calculated from the relation

$$\Delta G^0 = RT \ln K_d \tag{7}$$

3. Results

In our experiments, we examined the effect of TNP–ATP on the assembly of microtubules. Results show that TNP–ATP inhibits the polymerization of tubulin.

Figure 1 (curve a) shows polymerization of tubulin (2.6 mg/ml) in the presence of 1.3 mM ATP and in the absence of TNP–ATP. The ex-

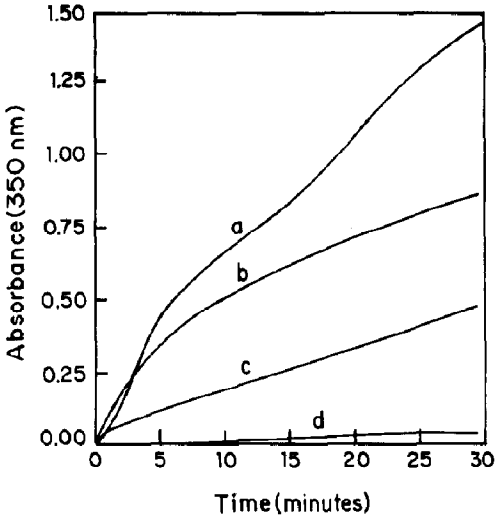

Fig. 1. Effect of TNP–ATP on tubulin polymerization. Polymerization of tubulin (2.6 mg/ml) in the assembly buffer (10 m*M* Pipes, pH 6.4, 5 m*M* $MgCl_2$, 1 m*M* EGTA, 3.4 *M* glycerol) was measured by turbidimetry (a) in the absence of TNP–ATP and presence of 1.3 m*M* ATP, (b) in the presence of 0.6 m*M* TNP–ATP and 1.3 m*M* ATP, (c) in the presence of 1.3 m*M* TNP–ATP and 1.3 m*M* ATP, and (d) in the presence of 0.6 m*M* TNP–ATP and in the absence of ATP.

tent of polymerization decreases with increasing TNP–ATP concentration while keeping the protein and ATP concentration constant. At 0.6 m*M* TNP–ATP, the polymerization is 60% (curve b) and at 1.3 m*M* TNP–ATP, the polymerization is 32% (curve c) of that obtained in the absence of the analogue. Curve d of Fig. 1 shows the effect of 0.6 m*M* TNP–ATP on the polymerization of tubulin in the absence of ATP. Further increase in the concentration of TNP–ATP does not have any effect on polymerization (data not shown). Polymerized protein depolymerizes upon cooling as revealed by the decrease in the absorbance at 350 nm to its original value.

These experiments clearly show that TNP–ATP does not induce tubulin self-assembly but inhibits the ATP induced assembly. The extent of inhibition increases with the increase of TNP–ATP concentration.

3.1. Fluorescence properties of TNP–ATP bound to tubulin

The binding of TNP–ATP to tubulin is reflected in the enhancement of the fluorescence intensity of TNP–ATP which can be used to monitor the interaction of the analogue with tubulin and obtain the binding parameters that characterize this interaction. Figure 2 shows fluorescence emission spectra of the free (a) and tubulin-bound (b) TNP–ATP. Blue shift from 555 to 530 nm in the fluorescence emission has been observed, indicating a decrease in the dielectric constant of the environment of the probe. This readily explains the increase in the fluorescence quantum yield. These results show that TNP–ATP binds to the hydrophobic region of the protein.

The dissociation constant for the tubulin–TNP–ATP complex (K_d) and maximum fluorescence of the bound probe were determined by the protein titration. The enhancement of the bound probe (Q) and binding constant were calculated from the double reciprocal plot (eq. 1) as shown in the Fig. 3. The enhancement factor (Q) was found to be 20 ± 1 and the dissociation constant for the TNP–ATP–protein complex was determined to be 110 ± 15 μM at 20°C.

The stoichiometry of TNP–ATP binding to tubulin was also determined by titration of tubulin with TNP–ATP and the results were plotted

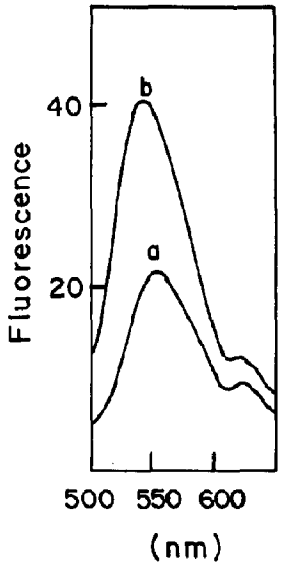

Fig. 2. Fluorescence emission spectra (uncorrected) of TNP–ATP. Fluorescence excitation was done at 480 nm and emission spectra were recorded of (a) TNP–ATP (5.5 μM) in 50 m*M* Pipes, pH 6.9, containing 1 m*M* EGTA, 23°C, and (b) after addition of tubulin (4.5 μM).

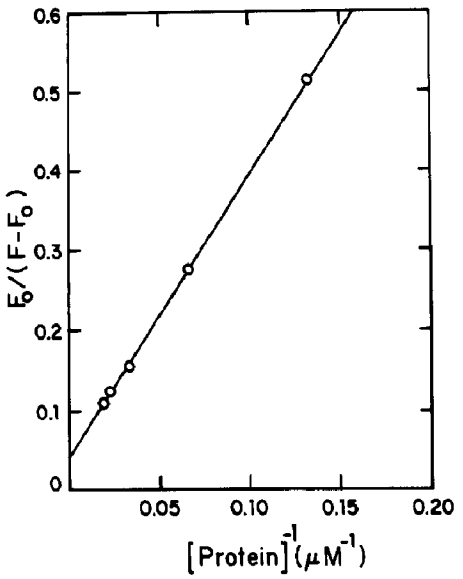

Fig. 3. Determination of the dissociation constant (K_d) of TNP–ATP–tubulin complex. The dissociation constant for TNP–ATP–tubulin complex was determined by protein titration of TNP–ATP fluorescence at 23°C, in 50 m*M* Pipes, pH 6.9, and 1 m*M* EGTA. Excitation emission wavelengths were 480 nm and 540 nm, respectively. Fluorescence enhancement by a factor of $Q = 20$ and K_d of 130 μM were obtained from the data plotted according to the eq. (1). The line is a least squares fit of the data and open circles denote experimental points. F and F_0 represent fluorescence intensity in the presence and absence of tubulin, respectively. The concentration of TNP–ATP was 12 μM, and protein concentration was varied form 7 to 34 μM.

according to the equation of Klotz (eq. 5). The plot of $1/\bar{\nu}$ vs. 1/[L] (Fig. 4) is a straight line. The intercept of the line gives the value of 1 binding site/mole and from the slope, the dissociation constant has been determined to be 95 ± 10 μM which is in agreement with the value determined from protein titration study as discussed above.

3.2. Temperature dependence of K_d

Figure 5 shows the plot of ln K_d as a function of temperature. The data can be fitted to a straight line (eq. 6) with $\Delta H^0 = -34.7 \pm 1.1$ kJ mol^{-1} and $\Delta S^0 = -41.00 \pm 7.1$ J K^{-1} mol^{-1}. The linear fit also shows that heat capacity change ΔC_p^0 for tubulin in the temperature range studied is nearly zero in agreement with other reports [17].

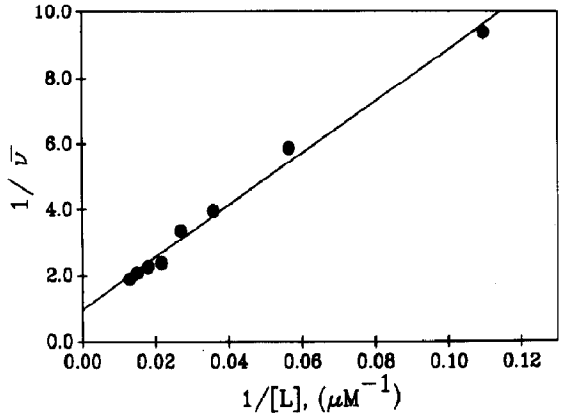

Fig. 4. Determination of the stoichiometry of TNP–ATP binding to tubulin. Stoichiometry of TNP–ATP binding to tubulin at 23°C was determined by a Klotz plot (eq. 5). Increasing concentrations of TNP–ATP were added to a 9.7 μM solution of tubulin in 50 m*M* Pipes, pH 6.9, and 1 m*M* EGTA. Nucleotide binding was followed by the fluorescence of the probe at 540 nm using an excitation wavelength of 520 nm. The straight line is a least squares fit of the data. The concentration of the bound ligand was determined according to the procedure described in Section 2.

Free energy change (ΔG^0) was calculated to be -22.2 ± 0.1 kJ mol^{-1} at 15°C and -21.4 ± 0.2 kJ mol^{-1} at 35°C. These values show that lower temperature favours binding.

3.3. Effect of nucleotide on TNP–ATP binding

In order to investigate possible relationship between the binding site of this analogue and

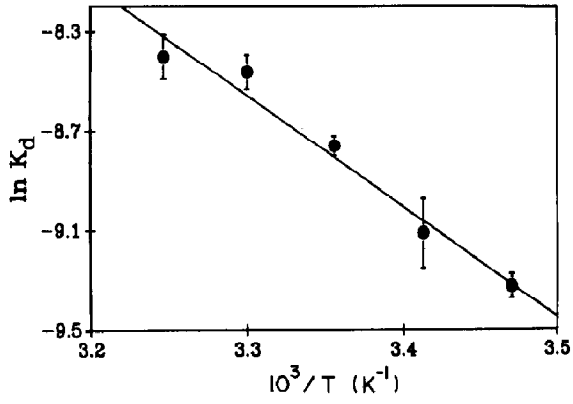

Fig. 5. Temperature dependence of the dissociation constant of TNP–ATP binding to tubulin. ΔH^0, ΔS^0 and ΔG^0 were obtained as described in section 2. Other experimental parameters are the same as in Fig. 3.

GTP or ATP binding site, the effect of GTP or ATP on the fluorescence of tubulin-bound TNP–ATP has been investigated. Addition of either GTP or ATP does not have any effect on the fluorescence of tubulin-bound TNP–ATP (not shown). When a concentration of ATP as high as 0.05 *M* ATP was added to a solution containing 8.5 μM tubulin and 14 μM TNP–ATP in the buffer, fluorescence intensity has not changed at all. Similarly GTP (0.05 M) also did not change the fluorescence of the tubulin-bound TNP–ATP. These results show that TNP–ATP does not bind at either ATP or GTP sites but binds at a site which may be a critical region for the assembly process.

3.4. Effect of metal ions on the fluorescence of bound TNP–ATP

It has been observed that Mg^{2+} decreases the fluorescence of tubulin-bound TNP–ATP. Increasing the concentration of Mg^{2+} decreases the fluorescence of tubulin-bound TNP–ATP (Fig. 6). Fluorescence of free TNP–ATP was not affected by the added metal ions. Protein titration was done in the absence and presence of Mg^{2+} ions (Fig. 6, inset). The results show that in the presence of 0.5 m*M* Mg^{2+}, the dissociation constant is 196 μM as compared to that in the absence of metal ions ($K_d = 95$ μM). However, the Q (enhancement factor) remains the same in the absence and presence of metal ions. These results show that the observed decrease in fluorescence intensity by the addition of $MgCl_2$ is not due to the conformational change caused by the metal ions at the TNP–ATP binding site. From Fig. 6, (inset) it is clear that Mg–TNP–ATP has a lower affinity to tubulin as compared to TNP–ATP. From the Mg^{2+} titration data, the stability constant of Mg^{2+}–TNP–ATP was found out to be 1.5×10^4 M^{-1}.

3.5 Effect of ANS on tubulin bound TNP–ATP

ANS and bis-ANS are good fluorescent probes for hydrophobic regions on the protein. Bis-ANS binds strongly to tubulin and is a potent inhibitor of tubulin assembly. Less strongly binding ANS

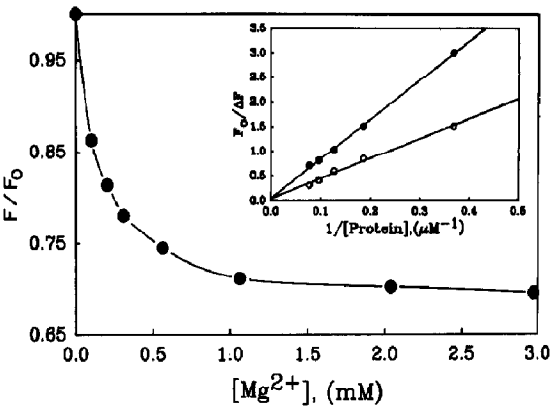

Fig. 6. Effect of Mg^{2+} on the fluorescence of TNP–ATP in the presence of tubulin. TNP–ATP fluorescence at 540 nm was monitored in the presence of varying concentration of Mg^{2+}. The cuvettes contained 15 μM tubulin and 14 μM TNP–ATP in 50 m*M* Pipes, pH 6.9, 1 m*M* EGTA, 23°C. F and F_0 are the fluorescence intensities of TNP–ATP–tubulin complex in the presence and absence of Mg^{2+}. (Inset) Titration of TNP–ATP with tubulin in the absence (open symbols) and in the presence of 0.54 m*M* Mg^{2+} (filled symbols). Solution contained 14 μM TNP–ATP in 50 m*M* Pipes, pH 6.9, 1 m*M* EGTA, 23°C. F_0 is the fluorescence intensity of TNP–ATP in the absence of protein. ΔF is the difference in the fluorescence intensity of TNP–ATP in the presence and absence of protein.

does not inhibit the tubulin assembly [18]. Both the dyes bind at a particular region. The region where bis-ANS binds to tubulin molecule is likely to be directly involved in microtubule assembly. In order to avoid the conformational change caused by bis-ANS, ANS was chosen to investigate the effect on TNP-ATP binding.

Fluorescence of TNP–ATP bound to tubulin was quenched by the addition of ANS while the fluorescence of free TNP–ATP was not. Stern–Volmer plot (Fig. 7) bends towards the x-axis showing that there are two kinds of TNP–ATP, one of which is quenched by the ANS and the other is not. These two species must be bound and free TNP–ATP, respectively. In such cases, the modified Stern–Volmer relation of Lehrer [19] is given by

$$\frac{F_0}{\Delta F} = \frac{1}{f_a K}\frac{1}{[A]} + \frac{1}{f_a}, \qquad (8)$$

where f_a is the fraction of the initial fluorescence which is accessible to ANS, [A] is the concentra-

tion of ANS, F_0 is the fluorescence intensity in the absence of ANS, ΔF is the difference in fluorescence intensity in the absence and presence of ANS, and K is the Stern–Volmer quenching constant. A plot of $F_0/\Delta F$ vs. $1/[A]$ is a straight line with slope of $1/f_a K$ and intercept of $1/f_a$ (Fig. 7, inset). From this, Stern–Volmer quenching constant (K) was calculated. The intercept on the ordinate is 2.0 indicating that 50% of the total observed fluorescence is quenchable. The Stern–Volmer constant was found to be 2.2 $\times 10^3$ M^{-1}. The apparent binding constant of ANS was calculated which was found to be 0.45 mM. In order to see the effect of ANS on the binding affinity of TNP–ATP to tubulin, protein titrations (eq. 1) were carried out in the absence and presence of ANS. The results show that in the presence of ANS, affinity of TNP–ATP to tubulin has not changed much, but the fluorescence enhancement factor has reduced from 20 ± 1 to 10 ± 1 (Fig. 8). This data shows that binding

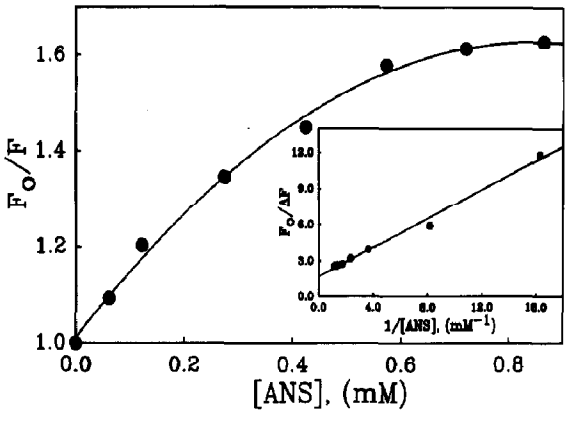

Fig. 7. Effect of ANS on the fluorescence of TNP–ATP in the presence of tubulin. TNP–ATP fluorescence intensity at 540 nm was monitored in the presence of varying concentration of ANS. The cuvettes contained 8 μM tubulin and 35 μM TNP–ATP in 50 mM Pipes, pH 6.9, 1 mM EGTA, 23°C. F and F_0 are the fluorescence intensities of TNP–ATP–tubulin complex in the presence and absence of ANS. (Inset) Modified Stern–Volmer plot (eq. 8) for the quenching of the fluorescence of TNP–ATP–tubulin complex by ANS. Tubulin (8 μM) in 50 mM Pipes, 1 mM EGTA, was titrated with increasing concentration of ANS and fluorescence intensity was measured at 540 nm. Excitation was at 480 nm. The corrected intensity was plotted as a function of the $[ANS]^{-1}$. The straight line is a least square fit of the data to eq. (8).

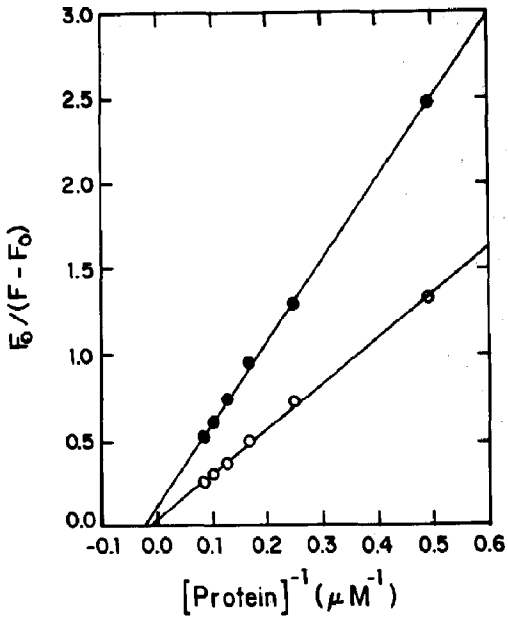

Fig. 8. Titration of TNP–ATP with tubulin in the absence and presence of ANS. TNP–ATP (6 μM) was titrated with protein in the absence (open symbol) and in presence (filled symbol of 0.4 mM ANS in 50 mM Pipes, pH 6.9, and 1 mM EGTA, at 23°C. Values for the maximum enhancement (Q) and K_d for the TNP–ATP–tubulin complex were obtained by a least squares fit of the data to the eq. (1) (see text).

of ANS to tubulin induces a local conformation change near the binding site of TNP–ATP, thereby reducing the quantum yield of bound TNP–ATP. It is known that, bis-ANS and ANS bind to a particular region of tubulin [20]. From these studies it is clear that TNP–ATP binding site must be located in the same region as that of bis-ANS and ANS.

3.6. Quenching of protein fluorescence by TNP–ATP

Quenching of intrinsic protein fluorescence gives information on the configuration of polypeptide chain. The protein exhibits characteristic fluorescence with maximal intensity at 330 nm when selectively excited at 295 nm for tryptophan. In tubulin, there are four tryptophan residues per subunit [21]. Contribution of tyrosine to protein fluorescence is reduced by shifting the excitation to 295 nm. Inner-filter effect due to the absorption of TNP–ATP at excitation wavelength

was corrected by estimation of the fluorescence quenching upon addition of TNP–ATP to L-tryptophan solution adjusted to give a fluorescence intensity equal to that obtained with the tubulin concentration used for the quenching study by TNP–ATP.

Protein fluorescence at 330 nm was quenched by the addition of TNP–ATP. The direct Stern–Volmer plot of the quenching data is an upward curvature, concave towards the y-axis (Fig. 9). This kind of plot shows that both dynamic and static quenching are taking place. The modified Stern–Volmer equation [22] in this case is given by

$$\frac{F_0}{Fe^{V[Q]}} = 1 + K_{sv}[Q], \qquad (9)$$

where K_{sv} is the dynamic quenching constant and V is the static quenching constant. Q is the concentration of TNP–ATP, F_0 and F are the fluorescence intensity of protein before and after adding the quencher, respectively. It is possible to fit the quenching data in eq. (9) by plotting $F_0/(F \exp(V[Q])$ vs. [Q] for varying V until a linear plot is obtained. The calculated value of K_{sv} and V are $3.5 \times 10^3\ M^{-1}$ and $9 \times 10^3\ M^{-1}$, respectively. From the quenching data, the binding constant of TNP–ATP to tubulin was calculated and was found to be 111 μM in agreement with the determination by other method at 23°C.

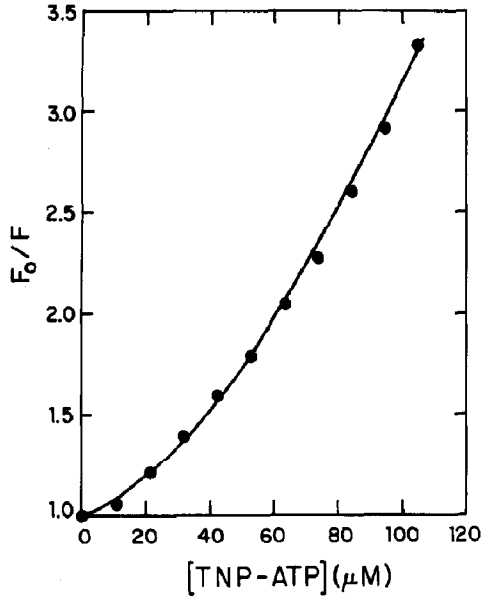

Fig. 9. Quenching of tubulin fluorescence by TNP–ATP. Solution containing tubulin (0.6 μM), in 50 mM Pipes, pH 6.9, and 1 mM EGTA, at 23°C was titrated with increasing concentration of TNP–ATP. Excitation was at 295 nm and emission at 330 nm. Measured fluorescence intensity was corrected for the absorption of TNP–ATP as described in text. F and F_0 are the fluorescence intensities of tubulin in the presence and absence of TNP–ATP, respectively.

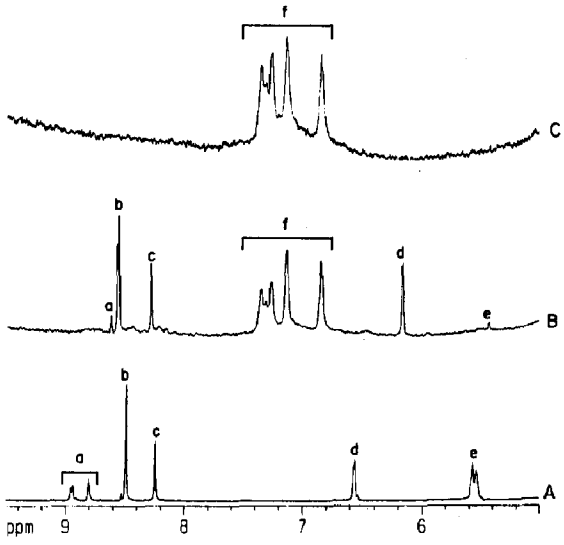

Fig. 10. NMR spectra of TNP–ATP–tubulin complex. All NMR spectra were taken in 20 mM Pipes, pH 7.0 in D_2O. (A) Portion of the NMR spectrum of pure TNP–ATP (5 mM) in the region 5–9.5 ppm. Proton resonances in the spectrum are assigned to (a) ring protons of trinitrophenyl group (peaks at 8.94 ppm, 8.8 ppm), (b) H_8 protons (peak at 8.49 ppm), (c) H_2 protons (peak at 8.24 ppm), (d) ribose protons, $H_{1'}$ (peak at 6.56 ppm), and (e) $H_{2'}$ protons (peak at 5.55 ppm). (B) Portion of NMR spectrum of TNP–ATP (5 mM) in the presence of tubulin (330 μM) in the same region as in (A). Notice that ring-proton resonances of trinitrophenyl group occur at (a) 8.62 ppm. The H_8 proton resonances occur at (b) 8.56 ppm and H_2 protons (c) at 8.28 ppm. The ribose protons, $H_{1'}$ (d) 6.16 ppm and $H_{2'}$ (e) at 5.43 ppm. (C) Portion of the NMR spectrum of tubulin alone (330 μM) in the same region as in (A) and (B). (f) is the aromatic region of the tubulin spectrum.

3.7. NMR study of TNP–ATP binding to tubulin

Figure 10(A) shows a portion of the proton NMR spectrum of pure TNP–ATP in the region of 5–9.5 ppm in 20 mM Pipes in D_2O, pH 7.0 at 23°C. Figure 10(B) shows the proton NMR spec-

trum of TNP–ATP recorded in the presence of tubulin under the same conditions as in (A). Figure 10(C) shows the proton NMR spectrum of tubulin alone in the same region shown for comparison. In the presence of tubulin (Fig. 10(B)), there is a change in the chemical shift in the various proton resonances of TNP–ATP. There is an upfield shift of about 0.3 ppm in the resonances of the protons of the trinitrophenyl ring. Similarly, an upfield shift of 0.4 ppm and 0.12 ppm has been observed for the ribose protons, $H_{1'}$ and $H_{2'}$ respectively. Further, there is a significant reduction in the intensity of the signal (e) due to the $H_{2'}$ protons of the sugar moiety. On the contrary, a small downfield shift of 0.07 ppm and 0.04 ppm has been observed for the base protons, H_8 and H_2, respectively. No chemical shift change has been observed for the aromatic protons of the protein arising from the mobile aromatic residues.

4. Discussion

The rationale for our studies on the interaction of TNP–ATP analogue with tubulin was to explore the possibility of using the fluorescence analogue of ATP to probe the binding site of ATP using fluorescence techniques and to characterize the interaction of TNP–ATP with tubulin in terms of the dissociation constant (K_d) and the stoichiometry of binding with tubulin. Our results indicate that TNP–ATP binds to the protein with a dissociation constant of $110 \pm 15\ \mu M$ at 23°C with a single binding site. Further, fluorescence experiments show that addition of ATP and GTP do not have any effect on the fluorescence intensity of tubulin-bound TNP–ATP implying that the binding site is different from that of ATP or GTP site. Also, CD spectra of tubulin recorded between 200 and 260 nm (not shown) were found to be identical in the presence and absence of the analogue suggesting that the binding of this nucleotide analogue does not cause any changes in the secondary structure of the protein.

TNP–ATP quenches 70% of the tryptophan fluorescence. Since protein fluorescence is quenched by static quenching, this suggests that TNP–ATP binds in the vicinity of tryptophan residues. It was reported that ANS has a specific binding site to tubulin (one binding site) [18,23]. Since ANS quenches the protein fluorescence, ANS binds to a site in the close vicinity of tryptophan residues [24]. Further, in our experiments we observed the quenching of the fluorescence of tubulin-bound TNP–ATP by ANS showing that ANS binding site is very near the TNP–ATP binding site residues. These results show that TNP–ATP binding site is in the vicinity of the ANS binding site and tryptophan residues. Brain tubulin has four tryptophan residues per subunit. Sequence studies have shown that three of these residues 21, 346, 407 are in the same position in both α and β subunits. Tryptophan residue at position 346 and 407 are likely to be closer to the subunit contact region [25] and are close to the cystein residue 354 which may be critical for assembly [26]. So it is likely that the TNP–ATP binding site is located in this region.

The temperature dependence of the K_d for TNP–ATP binding to tubulin yields negative values for both the enthalpy (ΔH^0) and entropy change (ΔS^0) (-34.7 kJ mol^{-1} and -41.0 J K^{-1} mol^{-1}, respectively). A negative value of entropy change suggests that tubulin–TNP–ATP complex attains a more ordered structure than the uncomplexed tubulin [27]. For a hydrophobic interaction both ΔH^0 and ΔS^0 are, in general, positive, yet in some cases it may give negative values [27]. Van der Waals interactions, hydrogen bond formation in low dielectric environments and ionic interaction make significant contributions to negative ΔH^0 and ΔS^0.

From NMR study, it appears that the trinitrophenyl ring interacts with the protein as is evident from the upfield shift of the aromatic ring protons of TNP–ATP. As a result of such interaction, it is possible that the deshielding effect of the nitro groups on trinitrophenyl ring protons and ribose protons is reduced resulting in an upfield shift of these protons in the presence of tubulin. The large upfield shift observed for the ribose protons, $H_{1'}$ and $H_{2'}$ as well as the dramatic reduction in the intensity of the signal due to the $H_{2'}$ protons shows the involvement of the

sugar moiety also in the interaction of TNP–ATP with tubulin. This reduction in the intensity of the NMR signal due to $H_{2'}$ proton results from extreme broadening of the signal. Infact, in some of the NMR spectra of TNP–ATP recorded in the presence of tubulin, this signal due to $H_{2'}$ protons disappears due to large broadening as a result of such interaction. A comparison of the spectra (B) and (C) shows that there is no change in the aromatic region of the protein spectrum arising due to mobile aromatic residues.

TNP–ATP is a competitive inhibitor of sodium and potassium ATPase [28] and DNA polymerase III holoenzyme [29]. The mode of inhibition by this analogue, however, seems to be different in the case of tubulin.

Our experiments show that TNP–ATP inhibits tubulin self-assembly by binding at a single site in the hydrophobic region in the vicinity of ANS and tryptophan residues but distinct from that of ATP. The present experiments with TNP–ATP nevertheless point out that modification at the 3′ position of the ribose of ATP inhibits polymerization.

Acknowledgments

The authors are grateful to Dr. B. Bhattacharyya of the Department of Biochemistry, Bose Institute, Calcutta, India for his invaluable advice and suggestions regarding the isolation and purification of tubulin. The authors also thank Ms. Kavita Kuchroo of our group for her help in the initial phase of this work. The authors thank the staff of the 500 MHz FT-NMR National facility of the help in using the NMR spectrometer.

References

1 M. Jacobs, H. Smith and E.W. Taylor, J. Mol. Biol. 89 (1974) 455.
2 R.C. Weisenberg, G.G. Borisy and E.W. Taylor, Biochemistry 7 (1968) 4466.
3 J.R. Zabrecky and R.D. Cole, J. Biol. Chem. 255 (1980) 11981.
4 J.R. Zabrecky and R.D. Cole, J. Biol. Chem. 257 (1982) 4633.
5 K. Islam and R.G. Burns, FEBS Lett. 178 (1984) 264.
6 J.R. Zabrecky and R.D. Cole, Arch. Biochem. Biophys. 225 (1983) 475.
7 C. Duanmu, C.M. Lin and E. Hamel, Biochim. Biophys. Acta, 881 (1986) 113.
8 T. Watanabe and G. Inesi, J. Biol. Chem. 257 (1982) 11510.
9 T. Hiratsuka, Biochim. Biophys. Acta. 453 (1976) 293.
10 K. Inaba, M. Okuno and H. Mohri, Arch. Biochem. Biophys. 274 (1989) 209.
11 R.S. Sarfati, V.K. Kansal, H. Munier, P. Glaser, A. Gilles, E. Labruyere, M. Mock, A. Danchin and O. Barzu, J. Biol. Chem. 265 (1990) 18902.
12 M.L. Shelanski, F. Gaskin and C.R. Cantor, Proc. Natl. Acad. Sci. U.S.A. 70 (1973) 765.
13 O.H. Lowry, N.J. Rosebrough, A.L. Farr and R.J. Randall, J. Biol. Chem. 193 (1951) 265.
14 T. Hiratsuka and K. Uchida, Biochim. Biophys. Acta. 320 (1973) 635.
15 J.R. Lakowicz, Principles of fluorescence spectroscopy (Plenum Press, New York, 1983) pp 1–44.
16 I.M. Klotz, Arch. Biochem. Biophys. 9 (1946) 109.
17 J. Robinson and Y. Engelborghs, J. Biol. Chem. 257 (1982) 5367.
18 P. Horowitz, V. Prasad and R.F. Luduena, J. Biol. Chem. 259 (1984) 14647.
19 S.S. Lehrer, Biochemistry 10 (1971) 3254.
20 A.R.S. Prasad, R.F. Luduena and P.M. Horowitz, Biochemistry 25, (1986) 3536.
21 E. Krauhs, M. Little, T. Kempf, R. Hofer-Warbinek, W. Ade and H. Ponstingl, Proc. Natl. Acad. Sci. U.S.A. 78 (1981) 4156.
22 M.R. Eftink and C.H. Ghiron, J. Phys. Chem. 80 (1976) 486.
23 B. Bhattacharyya and J. Wolff, Arch. Biochem. Biophys. 167 (1975) 264.
24 M. Steiner, Biochemistry 19 (1980) 4492.
25 H. Ponstingl, E. Krauhs, M. Little and T. Kempf, Proc. Natl. Acad. Sci. U.S.A. 78 (1981) 2757.
26 M. Little and R.F. Luduena, EMBO J. 4 (1985) 51.
27 P.D. Ross and S. Subramanian, Biochemistry 20 (1981) 3096.
28 E.G. Moczydlowski and P.A. George Fortes, J. Biol. Chem. 256 (1981) 2357.
29 R. Oberfelder and C.S. McHenry, J. Biol. Chem. 262 (1987) 4190.